Hindawi
Wireless Communications and Mobile Computing
Volume 2019, Article ID 9082362, 11 pages
https://doi.org/10.1155/2019/9082362

Research Article

Blind Fuzzy Adaptation Step Control for a Concurrent Neural Network Equalizer

Kayol S. Mayer[1] **Matheus S. De Oliveira**[2] **Candice Müller,**[3] **Fernando C. C. De Castro**[2] **and Maria C. F. De Castro**[2]

[1] *Department of Communications, University of Campinas, Campinas, SP, Brazil*
[2] *School of Technology, Pontifícia Universidade Católica do Rio Grande do Sul, Porto Alegre, RS, Brazil*
[3] *Technology Center, Universidade Federal de Santa Maria, Cidade Universitária, RS, Brazil*

Correspondence should be addressed to Kayol S. Mayer; kayol@decom.fee.unicamp.br

Received 27 September 2018; Revised 11 November 2018; Accepted 2 December 2018; Published 10 January 2019

Academic Editor: José A. García-Naya

Mobile communications, not infrequently, are disrupted by multipath propagation in the wireless channel. In this context, this paper proposes a new blind concurrent equalization approach that combines a Phase Transmittance Radial Basis Function Neural Network (PTRBFNN) and the classic Constant Modulus Algorithm (CMA) in a concurrent architecture, with a Fuzzy Controller (FC) responsible for adapting the PTRBFNN and CMA step sizes. Differently from the Neural Network (NN) based equalizers present in literature, the proposed Fuzzy Controller Concurrent Neural Network Equalizer (FC-CNNE) is a completely self-taught concurrent architecture that does not need any training. The Fuzzy Controller inputs are based on the estimated mean squared error of the equalization process and on its variation in time. The proposed solution has been evaluated over standard multipath VHF/UHF channels defined by the International Telecommunication Union. Results show that the FC-CNNE is able to achieve lower residual steady-state MSE value and/or faster convergence rate and consequently lower Bit Error Rate (BER) when compared to Constant Modulus Algorithm-Phase Transmittance Radial Basis Function Neural Network (CMA-PTRBFNN) equalizer.

1. Introduction

Digital communication over wireless channels may suffer severe signal distortion due to occurrence of multipath along the transmission channel. Not infrequently, nonlinearities at the receiver analog front-end and at the transmitter high power amplifier also impose distortions on the transmitted and received signals. Furthermore, the effects of all these impairments are worsened by the presence of additive white Gaussian noise (AWGN) [1–3].

Multipath arises, perhaps, as the most relevant impairment in digital wireless links [4]. Multipath propagation may cause Intersymbol Interference (ISI) [5], compromising the received signal intelligibility. Multipath effects are mitigated by means of channel equalization techniques [6], which basically implement the deconvolution of the channel impulse response [7].

In a general sense, channel equalizers can be divided into two categories: blind and nonblind equalizers [8]. Nonblind equalizers are inefficient in terms of data rate, since they require the transmission of a training sequence known by the receiver. In this context, blind equalizers [9] arise as an option to avoid waste of bandwidth, as they do not require any training sequence to achieve satisfactory convergence. Constant Modulus Algorithm (CMA) [10] is one of the most used algorithms for adaptive blind equalizers in Quadrature Amplitude Modulation (QAM) [11].

Nevertheless, CMA algorithm has a drawback: a CMA based equalizer presents moderate residual Mean Squared Error (MSE) after convergence [4, 9]. In [9], De Castro et al. proposed a concurrent blind channel deconvolution algorithm to circumvent this issue. The concurrent equalizer is composed by the CMA and by the Direct Decision (DD) [12] algorithms operating in a concurrent architecture. This proposed architecture increases the equalizer performance when compared to conventional CMA [9].

In [2], a concurrent blind equalizer architecture based on CMA algorithm and a complex Radial Basis Function

(RBF) neural network, called Phase Transmittance Radial Basis Function Neural Network (PTRBFNN), was presented as CMA-PTRBFNN. This CMA-PTRBFNN treats linear and nonlinear channels, keeping the input signal phase information. Thus, it is able to cope with the nonlinearities that usually occur at the transmitter power amplifier and at the receiver analog front-end. As shown in [2], this approach is able to reduce the residual steady-state MSE after convergence even when the receiver RF front-end operates near the upper limit of its dynamic range, situation that distorts the received signal. Such distortion, in the demodulated signal, usually occurs due to nonlinear transmittances at the analog blocks of the receiver RF front-end [2, 3].

In a broad sense, adaptive blind channel equalization aims to achieve two main goals: fast convergence rate and low residual steady-state MSE after convergence [2, 4, 13], which, in most cases, leads to a lower BER (Bit Error Rate), although BER and MSE are not necessarily related [14]. Achieving both goals is not a simple task, particularly for channels with significant echoes and long path delays. In order to reduce the residual steady-state MSE, a smaller adaptation step value is required, but it will slow down the equalizer convergence rate. On the other hand, to achieve faster convergence, a larger adaptation step value is necessary. However, a larger adaptation step will also result in a larger residual MSE and possibly a higher chance of instability [15].

In [6], Das proposed a complex fuzzy system for adapting the multi-level sigmoid function of a Decision Feedback Equalizer (DFE). This architecture reduced the bit error rate and presented a fast convergence rate. Hu et al. proposed the Simplified Fuzzy Stochastic Gradient (SFGF) to improve MSE performance [15] with satisfactory convergence rate. For subband adaptive channel equalization, Ng et al. proposed the Block-based Fuzzy Step Size (BFSS) strategy for the Normalized Least Mean Square (NLMS) algorithm. The BFSS updates the adaptation step over fixed time intervals in order to reduce computational complexity without sacrificing convergence rate and MSE performance [16]. The main drawback of SFGF and BFSS algorithms is the necessity to transmit a training sequence, which is used to update the adaptation step [15, 16].

In this context, this paper proposes a blind equalization approach that combines a Phase Transmittance Radial Basis Function Neural Network and the classic CMA algorithm in a concurrent architecture, with a Fuzzy Controller (FC) responsible for adapting the PTRBFNN and CMA step sizes. Differently from the Neural Network (NN) based equalizers present in literature, the proposed fuzzy controlled concurrent equalizer, called FC-CNNE, is a completely self-taught concurrent architecture that does not need any training. The Fuzzy Controller inputs are based on the estimated mean squared error of the equalization process and on its variation in time. With the continuous adjustment of the step sizes, the proposed approach is able to achieve lower residual steady-state MSE, lower BER, and/or faster convergence rate, when compared to CMA-PTRBFNN.

The remaining of this paper is organized as follows. Section 2 briefly describes the CMA-PTRBFNN architecture. In Section 3, the main contribution of this paper is presented: the proposed FC algorithm for the FC-CNNE. In Section 4, the performance of the proposed equalizer is presented. Simulation results of FC-CNNE are compared to results obtained by CMA-PTRBFNN, considering several benchmark multipath channel models. Section 5 concludes the paper, summarizing the main ideas and results presented in this work.

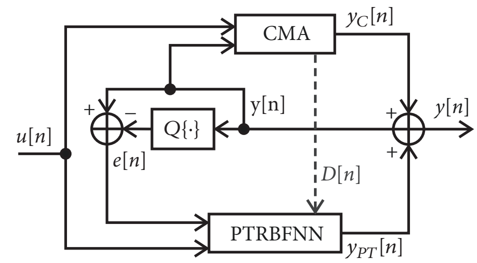

Figure 1: Constant Modulus Algorithm-Phase Transmittance Radial Basis Function Neural Network (CMA-PTRBFNN) proposed by Loss *et al.* [2].

2. Constant Modulus Algorithm-Phase Transmittance Radial Basis Function Neural Network (CMA-PTRBFNN)

The CMA-PTRBFNN combines the CMA algorithm and a Phase Transmittance Radial Basis Function Neural Network [2]. Figure 1 presents the equalizer block diagram. Complex baseband samples received from the channel are stored in a FIFO buffer of length L called channel regressor. Channel regressor is here represented by $\mathbf{u} = [u_0\ u_1\ \cdots\ u_{L-1}]^T$ vector, where T denotes the transpose operator. Both CMA and PTRBFNN blocks receive as input the channel regressor $\mathbf{u}$.

The CMA-PTRBFNN output $y[n]$ is obtained by the summation of CMA filter output $y_c[n]$ and PTRBFNN output $y_{PT}[n]$, as shown in Figure 1, and given by

$$y[n] = y_c[n] + y_{PT}[n]. \quad (1)$$

The CMA block output is obtained by

$$y_c[n] = \sum_{l=0}^{L-1} v_l[n]\, u_l[n], \quad (2)$$

where u_l is the l^{th} component of the channel regressor $\mathbf{u}$ and v_l is the l^{th} component of $\mathbf{v} = [v_0\ v_1\ \cdots\ v_{L-1}]^T$. $\mathbf{v}$ is the vector that represents the CMA FIR filter coefficients, which is adjusted by the Godard cost function [10].

The CMA coefficients update is given by

$$\mathbf{v}[n+1] = \mathbf{v}[n] + y[n]\,\eta_v\left(\gamma - |y[n]|^2\right)\mathbf{u}^*[n], \quad (3)$$

where $*$ is the complex conjugate operator, η_v is the adaptation step, and γ is the dispersion constant defined as

$$\gamma = \frac{\mathrm{E}\left\{|A|^4\right\}}{\mathrm{E}\left\{|A|^2\right\}}, \quad (4)$$

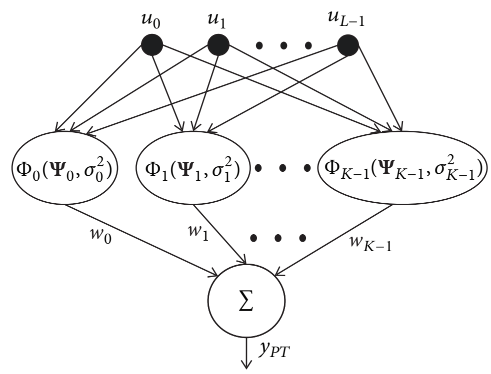

Figure 2: PTRBFNN architecture proposed by Loss *et al.* [2].

with E{·} being the expectation operator and A the set of digital IQ symbols of the reference constellation. For example, a 16-QAM modulation with a unit variance alphabet has $\gamma = 1.32$.

The PTRBFNN block output is obtained by

$$y_{PT}[n] = \sum_{k=0}^{K-1} w_k[n]\,\Phi_k[n], \tag{5}$$

with K being the number of neurons of the PTRBFNN block, where each neuron represents a Gaussian center, as shown in Figure 2. w_k is the k^{th} component of the complex valued synaptic weights vector $\mathbf{w} = \begin{bmatrix} w_0 & w_1 & \cdots & w_{K-1} \end{bmatrix}^T$ and Φ_k is the output of the k^{th} neuron, given by

$$\Phi_k = \exp\left(-\frac{\left\|\operatorname{Re}\{\mathbf{u}\} - \operatorname{Re}\{\mathbf{\Psi}_k\}\right\|_2^2}{\operatorname{Re}\{\sigma_k^2\}}\right) + j\exp\left(-\frac{\left\|\operatorname{Im}\{\mathbf{u}\} - \operatorname{Im}\{\mathbf{\Psi}_k\}\right\|_2^2}{\operatorname{Im}\{\sigma_k^2\}}\right), \tag{6}$$

where Re{·} and Im{·} are the real and imaginary operators, respectively. $\mathbf{\Psi}_k$ is the k^{th} center vector of $\mathbf{\Xi} = \begin{bmatrix} \mathbf{\Psi}_0 & \mathbf{\Psi}_1 & \cdots & \mathbf{\Psi}_{K-1} \end{bmatrix}^T$ associated with the k^{th} Gaussian center with variance σ_k^2.

The update of the PTRBFNN block free parameters (w_k, $\mathbf{\Psi}_k$, and σ_k^2) is controlled by $D[n]$ function, as follows:

$$D[n] = \begin{cases} 1, & Q\{y[n]\} = Q\{\tilde{y}[n]\} \\ 0, & Q\{y[n]\} \neq Q\{\tilde{y}[n]\}, \end{cases} \tag{7}$$

where the operator $Q\{\tilde{y}[n]\}$ returns the reference constellation IQ symbol with smallest Euclidean distance from its argument {·} and $\tilde{y}[n]$ is the CMA-PTRBFNN output after update of the CMA filter coefficients $\mathbf{v}$ by (3). Thus, $\tilde{y}[n]$ is obtained by

$$\tilde{y}[n] = \mathbf{w}^T[n]\,\mathbf{\Phi}[n] + \mathbf{v}^T[n+1]\,\mathbf{u}[n]. \tag{8}$$

According to (7), if $D[n] = 1$, the CMA-PTRBFNN output $y[n]$ and its updated version $\tilde{y}[n]$ resulted in the same IQ symbol. In this case, the PTRBFNN block free parameters are updated. Otherwise, if $D[n] = 0$, free parameters are not updated.

The free parameters of the PTRBFNN block are updated as follows:

$$\begin{aligned} \mathbf{\Psi}_k[n+1] &= \mathbf{\Psi}_k[n] + \eta_\Psi D[n] \\ &\quad\cdot\left(\operatorname{Re}\{\mathbf{\Theta}_k[n]\}\,\xi_k[n] + \operatorname{Im}\{\mathbf{\Theta}_k[n]\}\,\rho_k[n]\right), \\ \sigma_k^2[n+1] &= \sigma_k^2[n] + \frac{\eta_{\sigma^2}}{2}D[n] \\ &\quad\cdot\left(\operatorname{Re}\{\zeta_k[n]\}\,\xi_k[n] + \operatorname{Im}\{\zeta_k[n]\}\,\rho_k[n]\right), \\ \mathbf{w}[n+1] &= \mathbf{w}[n] + \eta_w D[n]\,e[n]\,\mathbf{\Phi}^*[n], \end{aligned} \tag{9}$$

where $e[n] = Q\{y[n]\} - y[n]$ is the error signal. η_Ψ, η_{σ^2}, and η_w are the adaptive steps of the center vectors $\mathbf{\Psi}_k$, variances σ_k^2, and synaptic weights w_k, respectively. $\mathbf{\Theta}_k$, ζ_k, ξ_k, and ρ_k are auxiliary variables used in order to simplify the PTRBFNN equations. These variables are defined by the following relations:

$$\begin{aligned} &\mathbf{\Theta}_k[n] \\ &\quad= \frac{\operatorname{Re}\{\Phi_k[n]\}\left(\operatorname{Re}\{\mathbf{u}[n]\} - \operatorname{Re}\{\mathbf{\Psi}_k[n]\}\right)}{\operatorname{Re}\{\sigma_k^2[n]\}} \\ &\qquad + j\frac{\operatorname{Im}\{\Phi_k[n]\}\left(\operatorname{Im}\{\mathbf{u}[n]\} - \operatorname{Im}\{\mathbf{\Psi}_k[n]\}\right)}{\operatorname{Im}\{\sigma_k^2[n]\}}, \end{aligned} \tag{10}$$

$$\begin{aligned} &\zeta_k[n] \\ &\quad= \frac{\operatorname{Re}\{\Phi_k[n]\}\left\|\operatorname{Re}\{\mathbf{u}[n]\} - \operatorname{Re}\{\mathbf{\Psi}_k[n]\}\right\|_2^2}{\left(\operatorname{Re}\{\sigma_k^2[n]\}\right)^2} \\ &\qquad + j\frac{\operatorname{Im}\{\Phi_k[n]\}\left\|\operatorname{Im}\{\mathbf{u}[n]\} - \operatorname{Im}\{\mathbf{\Psi}_k[n]\}\right\|_2^2}{\left(\operatorname{Im}\{\sigma_k^2[n]\}\right)^2}, \end{aligned} \tag{11}$$

$$\xi_k[n] = w_k^*[n]\,e[n] + w_k[n]\,e^*[n], \tag{12}$$

$$\rho_k[n] = w_k^*[n]\,e[n] - w_k[n]\,e^*[n]. \tag{13}$$

3. Blind Fuzzy Adaptation Step Control for the Concurrent Neural Network Equalizer

In the CMA-PTRBFNN presented in Section 2, the adaptation steps, i.e., η_v, η_Ψ, η_{σ^2}, and η_w, are constant values. They are defined aiming to achieve satisfactory trade-off between fast convergence and low residual steady-state MSE.

This paper proposes a Blind Fuzzy Adaptation Step control in order to iteratively adjust the CNNE adaptation steps, so that an improvement of the CMA-PTRBFNN performance in terms of convergence rate and/or residual mean squared error is achieved. Blind fuzzy adaptation step control algorithm is based on a fuzzy controller [17]. The proposed architecture of the FC-CNNE is shown in Figure 3. Note that it receives two input signals: $E[n]$ the estimated MSE and $\Delta E[n]$ the estimated MSE variation.

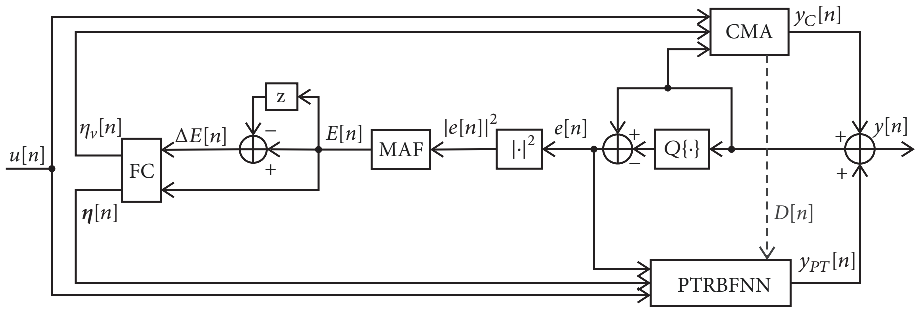

Figure 3: FC-CNNE block diagram.

Table 1: Fuzzy rules base.

Estimated MSE $E[n]$	Estimated MSE variation $\Delta E[n]$ LN	MN	SN	ZE	SP	MP	LP
VL	ME	ME	PL	PL	LO	LO	VL
LO	PH	PH	ME	ME	PL	PL	VL
PL	HI	PH	PH	ME	PL	PL	VL
ME	HI	HI	PH	HI	ME	VL	VL
PH	HI	HI	HI	VH	ME	VL	VL
HI	VH	VH	VH	VH	ME	VL	VL
VH	VH	VH	VH	VH	HI	VL	VL

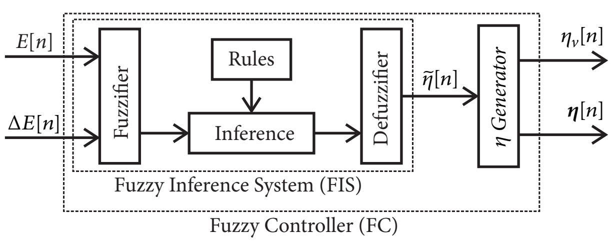

Figure 4: Details of the Fuzzy controller presented in Figure 3.

The estimated MSE is computed applying a Moving Average Filter (MAF) on the estimated instant square error $|e[n]|^2$. $E[n]$ is given by

$$E[n] = \frac{1}{P}\sum_{p=0}^{P-1} \left|e[n-p]\right|^2, \tag{14}$$

being P the filter window length.

The variation of the MSE is defined as

$$\Delta E[n] = E[n] - E[n-1]. \tag{15}$$

Figure 4 depicts the proposed fuzzy controller architecture, which uses the Mamdani inference method [18]. The FC outputs $\boldsymbol{\eta} = [\eta_w[n] \;\; \eta_\Psi[n] \;\; \eta_{\sigma^2}[n]]^T$ and $\eta_v[n]$ are applied to (3) and (9), respectively, adjusting the adaptive steps of FC-CNNE.

Fuzzy rules were defined in seven categories of linguistic variables, Very High (VH), High (HI), Partially High (PH), Medium (ME), Partially Low (PL), Low (LO), and Very Low (VL), aiming to obtain better partition of the universe of discourse. These linguistic variables are used to describe the fuzzifier input variable $E[n]$ and the defuzzifier output variable $\tilde{\eta}[n]$.

For the fuzzifier input variable $\Delta E[n]$, another seven categories of linguistic variables were defined: Large Positive (LP), Medium Positive (MP), Small Positive (SP), Zero (ZE), Small Negative (SN), Medium Negative (MN), and Large Negative (LN).

The Fuzzy controller membership functions are composed by triangular and trapezoidal distributions as can be seen in Figure 5. All curve parameters were defined according to a set of simulation tests and *a priori* knowledge about adaptation step influence in the stochastic gradient.

Table 1 presents the fuzzy inference engine rules for the membership functions shown in Figure 5. The fuzzy base presented in Table 1 constructs a set of "IF...THEN" rules. Since there are seven fuzzy sets for the inputs ($\Delta E[n]$ and $E[n]$) and output ($\tilde{\eta}[n]$), the number of statements is forty-nine.

Some examples of interpretations presented in Table 1 are listed as follows:

(i) IF $E[n]$ is VL and $\Delta E[n]$ is LN, THEN $\tilde{\eta}[n]$ is ME;

(ii) IF $E[n]$ is VL and $\Delta E[n]$ is MN, THEN $\tilde{\eta}[n]$ is ME;

(iii) ....

(iv) IF $E[n]$ is VH and $\Delta E[n]$ is LP, THEN $\tilde{\eta}[n]$ is VL.

Fuzzy controller implication and aggregation methods use the minimum operator. Defuzzification converts the aggregated fuzzy value to the adaptive step using the centroid technique, which returns the area center under the aggregated fuzzy value.

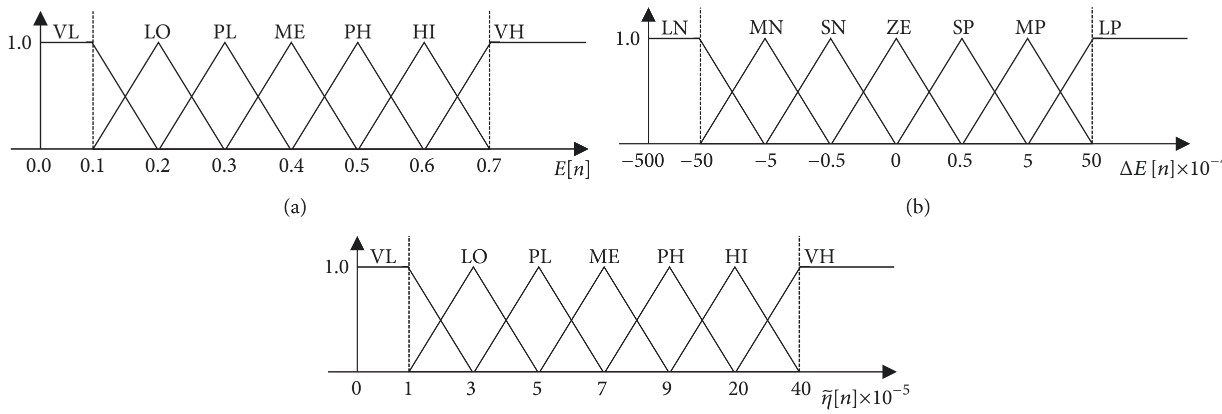

Figure 5: Membership Functions: (a) Input variable $E[n]$, (b) Input variable $\Delta E[n]$, (c) Output variable $\tilde{\eta}[n]$.

Table 2: Computational complexities.

Equalizer	Multiplications	Additions	exp(·) evaluations
CMA-PTRBFNN	$12KL + 12L + 30K + 7$	$14KL + 12L + 18K$	$2K$
FC-CNNE	$12KL + 12L + 30K + 117$	$14KL + 12L + 18K + P + 203$	$2K$

At the η *Generator* block, shown in Figure 4, the defuzzified output $\tilde{\eta}[n]$ is converted into CMA adaptive step $\eta_v[n]$ and into PTRBFNN adaptive step vector $\boldsymbol{\eta} = [\eta_w[n]\ \ \eta_\Psi[n]\ \ \eta_{\sigma^2}[n]]^T$. $\eta_v[n]$ and $\boldsymbol{\eta}[n]$ are applied to CMA and PTRBFNN blocks, respectively, as shown in Figure 3 and (3) and (9). CMA adaptation step is defined as $\eta_v[n] = \tilde{\eta}[n]$ and PTRBFNN adaptive step vector is defined as

$$\begin{aligned}\boldsymbol{\eta}[n] &= [\eta_w[n]\ \ \eta_\Psi[n]\ \ \eta_{\sigma^2}[n]]^T \\ &= [10\tilde{\eta}[n]\ \ 100\tilde{\eta}[n]\ \ 100\tilde{\eta}[n]]^T.\end{aligned} \tag{16}$$

Table 2 presents the CMA-PTRBFNN and the FC-CNNE computational complexities, recalling that L is the channel regressor size, K is the number of neurons, and P is the filter window length. Note that the FC-CNNE approach presents a minimally higher complexity.

4. Simulation Results

The proposed blind FC-CNNE equalizer has been implemented in C language. The equalizer has been evaluated with 16-QAM modulation, using an oversampling factor of two samples per symbol. The oversampling aims to avoid the noise enhancement effect on the equalizer performance that occurs when the equalizer is not fractionally spaced and the transmission channel presents zeros on the z-plane unit circle [19].

The proposed approach has been compared to CMA-PTRBNN presented in [2] over five VHF/UHF multipath scenarios, the so-called Brazil channels, standardized by the International Telecommunication Union (ITU) [20]. For the MSE simulations, AWGN with Signal-to-Noise Ratio (SNR) of 35 dB has been added in all evaluated scenarios. Figure 6 presents the impulse response of Brazil channels A, B, C, D, and E for two samples per symbol, where S_R is the symbol rate.

Both CMA-PTRBNN and FC-CNNE operate under the same conditions. Regressor size L is made equal to the delay spread resulting from the channel multipath scenario. The number of neurons adopted for the neural network is $K = 5$. For both equalizers, the initialization scheme is as follows:

(i) Initialization of the CMA filter coefficients follows the single spike method [21];

(ii) PTRBFNN synapses vector is initialized with $\mathbf{w}[0] = \mathbf{0} + \mathbf{j0}$;

(iii) The L components of the k^{th} center $\boldsymbol{\Psi}_k[0]$ are initialized by randomly drawing IQ symbols from the 16-QAM reference constellation;

(iv) The K values of $\sigma_k^2[0]$ are initialized with half of the maximum Euclidean distance among all respective vectors $\mathrm{Re}\{\boldsymbol{\Psi}_k[0]\}$ and $\mathrm{Im}\{\boldsymbol{\Psi}_k[0]\}$, with index $k = 0, 1, \ldots, K-1$.

For CMA-PTRBNN, the adaptation steps are defined as $\eta_v = 0.0001$, $\eta_w = 0.001$, $\eta_\Psi = 0.1$, and $\eta_{\sigma^2} = 0.1$. On the other hand, adaptation steps for FC-CNNE are adjusted at each iteration, as presented in Section 3. The performance is measured by means of the MSE filtered by the MAF with $P = 100$ coefficients.

Figure 7 presents results comparison between CMA-PTRBNN and FC-CNNE equalizers over the five multipath scenarios defined in Figure 6. Notice that, for all five evaluated channels, the FC-CNNE achieved better results.

For Brazil A channel (Figure 7(a)), FC-CNNE obtained faster convergence rate and similar residual error. A MSE of

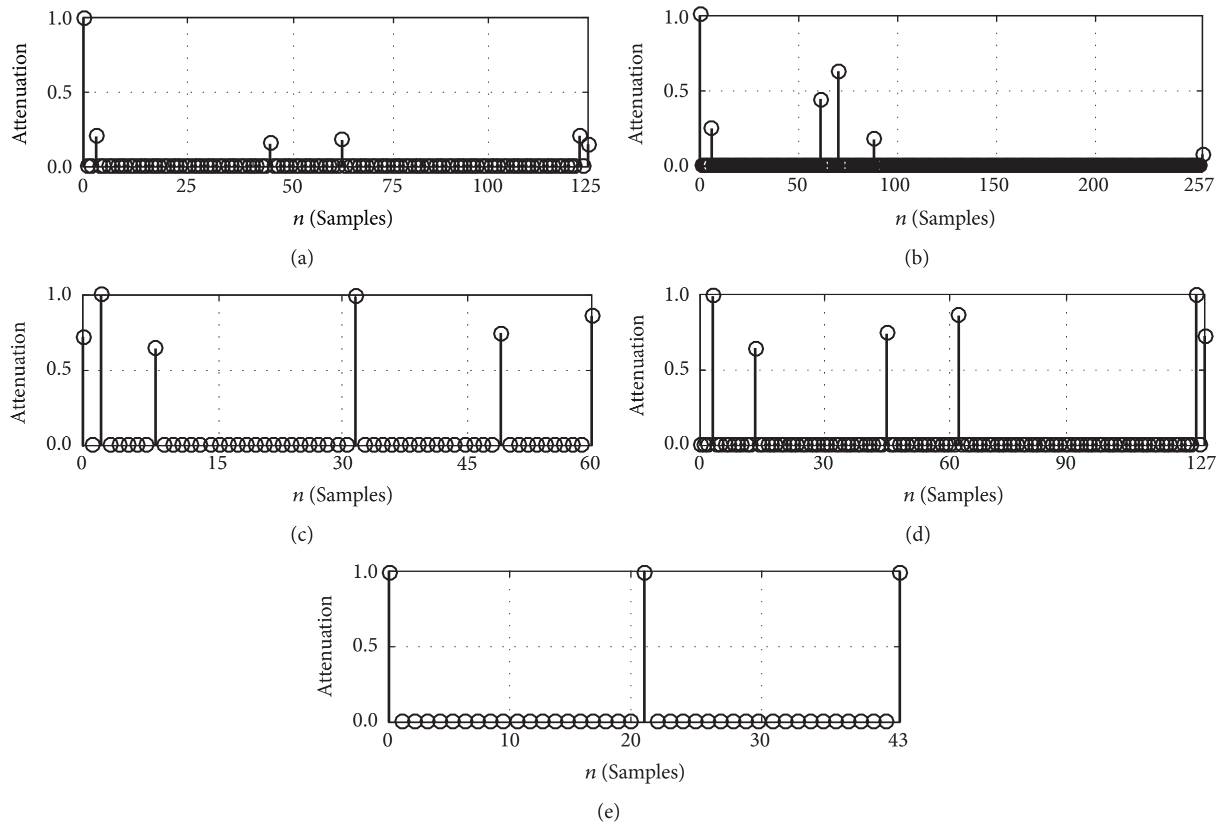

Figure 6: Impulse responses: (a) Brazil A channel, S_R = 10.5 MHz, (b) Brazil B channel, S_R = 10.1 MHz, (c) Brazil C channel, S_R = 10.7 MHz, (d) Brazil D channel, S_R = 10.7 MHz, and (e) Brazil E channel, S_R = 10.7 MHz.

0.10 is achieved after 5000 received symbols, while CMA-PTRBNN (with fixed step) achieved a MSE of 0.12. For channels Brazil B (Figure 7(b)), Brazil C (Figure 7(c)), and Brazil E (Figure 7(e)) the proposed equalizer obtained lower residual MSE and faster convergence rate compared to the fixed step algorithm. For Brazil D channel (Figure 7(d)), FC-CNNE yielded reduced residual MSE with similar convergence rate when compared to CMA-PTRBNN.

Figure 8 compares BER performance between CMA-PTRBNN and FC-CNNE equalizers, over the five Brazil channels. Through the set of results presented in Figures 7 and 8, it is possible to verify the correlation between MSE and BER. Note that, for Brazil A, both equalizers present similar residual MSE and, consequently, similar BER performance, while for the other evaluated channels, FC-CNNE achieved a lower residual MSE and, consequently, a lower BER.

As shown in Figure 6, Brazil D and Brazil E are the channels that present strongest echoes among the five evaluated multipath scenarios. Figure 9 presents CMA-PTRBFNN and FC-CNNE output constellations for these two scenarios, considering the last ten thousand IQ symbols. It is possible to see that, for both cases, the output constellation of the proposed equalizer presents smaller dispersion around the IQ symbols of the reference constellation when compared to CMA-PTRBFNN. Results for the remaining scenarios are presented in the Appendix.

Observe that, for 16-QAM modulation, the FC-CNNE yields a slightly better BER than the CMA-PTRBFNN for Eb/No > 17 dB, as shown in Figure 8. This just slightly better BER performance of the FC-CNNE stems from the somewhat large decision regions of the 16-QAM demapper. In fact, the dispersion of the received 16-QAM symbols around the reference symbols of the 16-QAM alphabet is noticeable smaller for the FC-CNNE, as shown in Figure 9, indicating an intrinsic lower MER (Modulation Error Ratio) [22] yielded by the FC-CNNE with respect to the CMA-PTRBFNN. Such smaller symbol dispersion, or MER, gives a superior operational margin for the FC-CNNE in dynamic scenarios, such as wireless mobile operation, in which the channel impulse response varies over time.

5. Conclusion

This paper presented a new blind concurrent equalizer approach, based on complex radial basis function neural networks and the CMA algorithm. The proposed approach applies a blind Fuzzy Controller, responsible for adapting the step size of both concurrent PTRBFNN and CMA algorithms. The fuzzy controller adjusts the adaptation steps based on the estimated mean squared error of the equalization process and on its variation in time. The fuzzy inference engine rules have

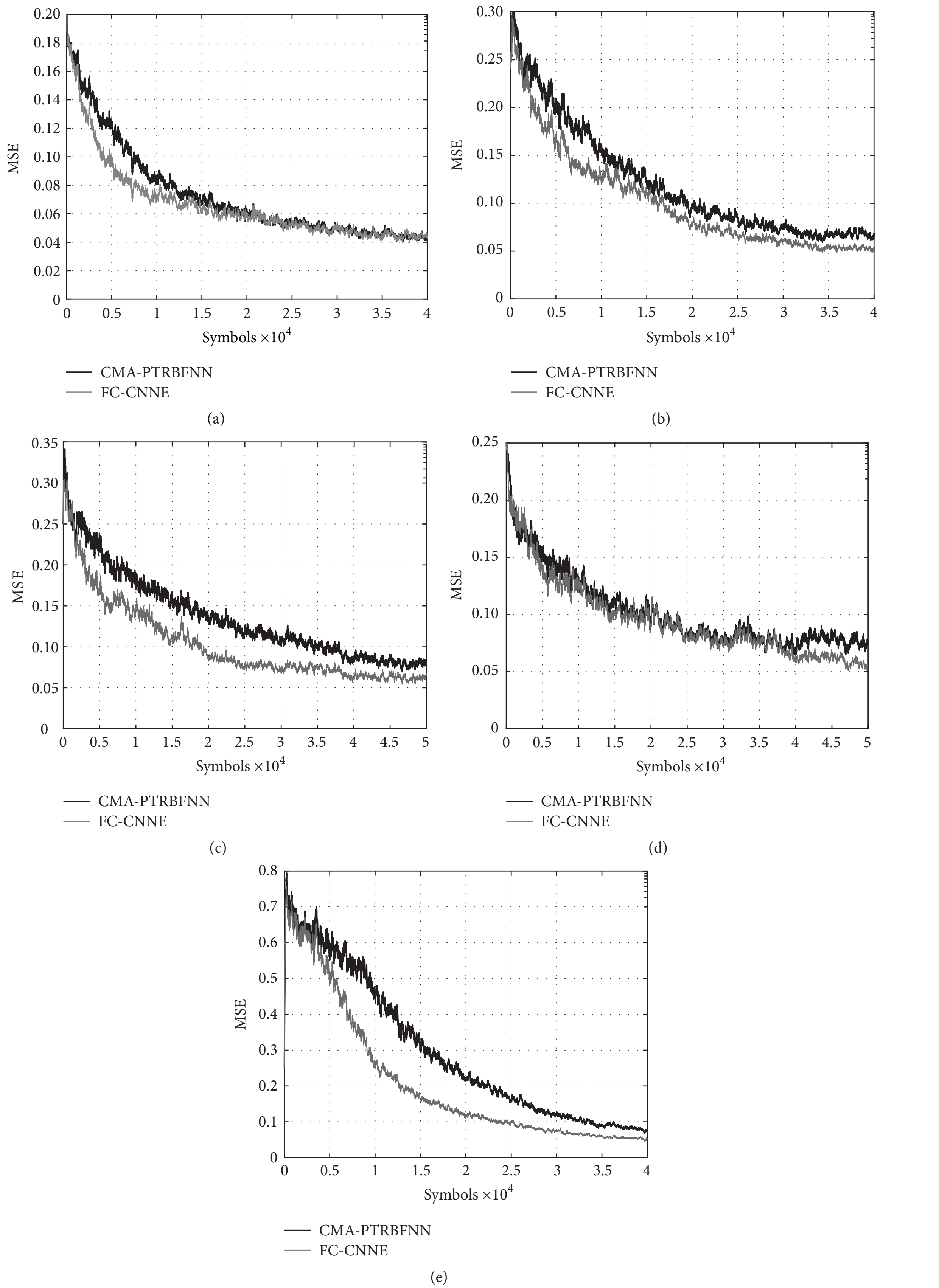

Figure 7: Comparison of simulation results obtained by the CMA-PTRBFNN and the FC-CNNE considering the five Brazil channel multipath scenarios: (a) Brazil A channel, $S_R = 10.5$ MHz, (b) Brazil B channel, $S_R = 10.1$ MHz, (c) Brazil C channel, $S_R = 10.7$ MHz, (d) Brazil D channel, $S_R = 10.7$ MHz, and (e) Brazil E channel, $S_R = 10.7$ MHz.

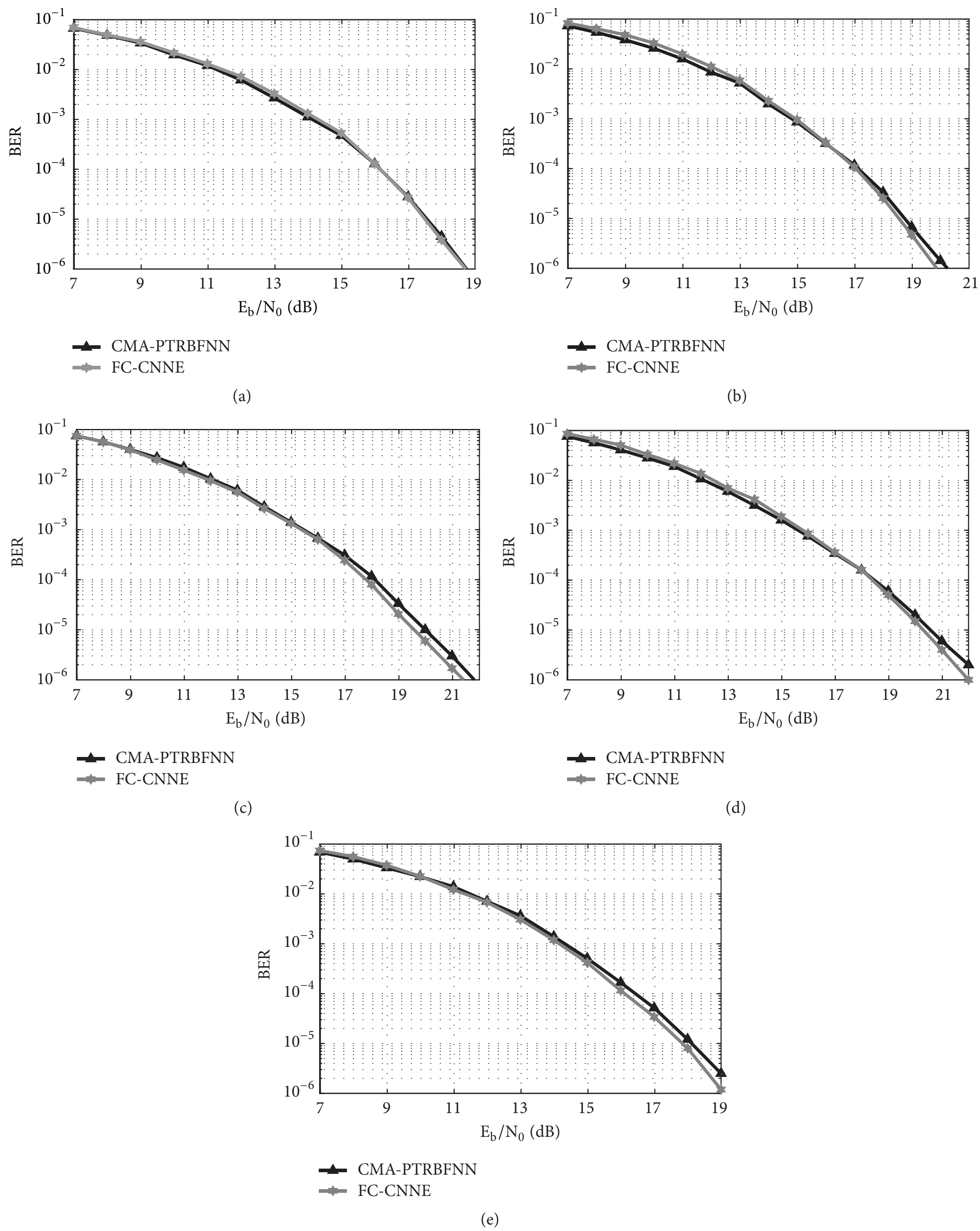

Figure 8: CMA-PTRBFNN and FC-CNNE BER performance: (a) Brazil A channel, (b) Brazil B channel, (c) Brazil C channel, (d) Brazil D channel, and (e) Brazil E channel.

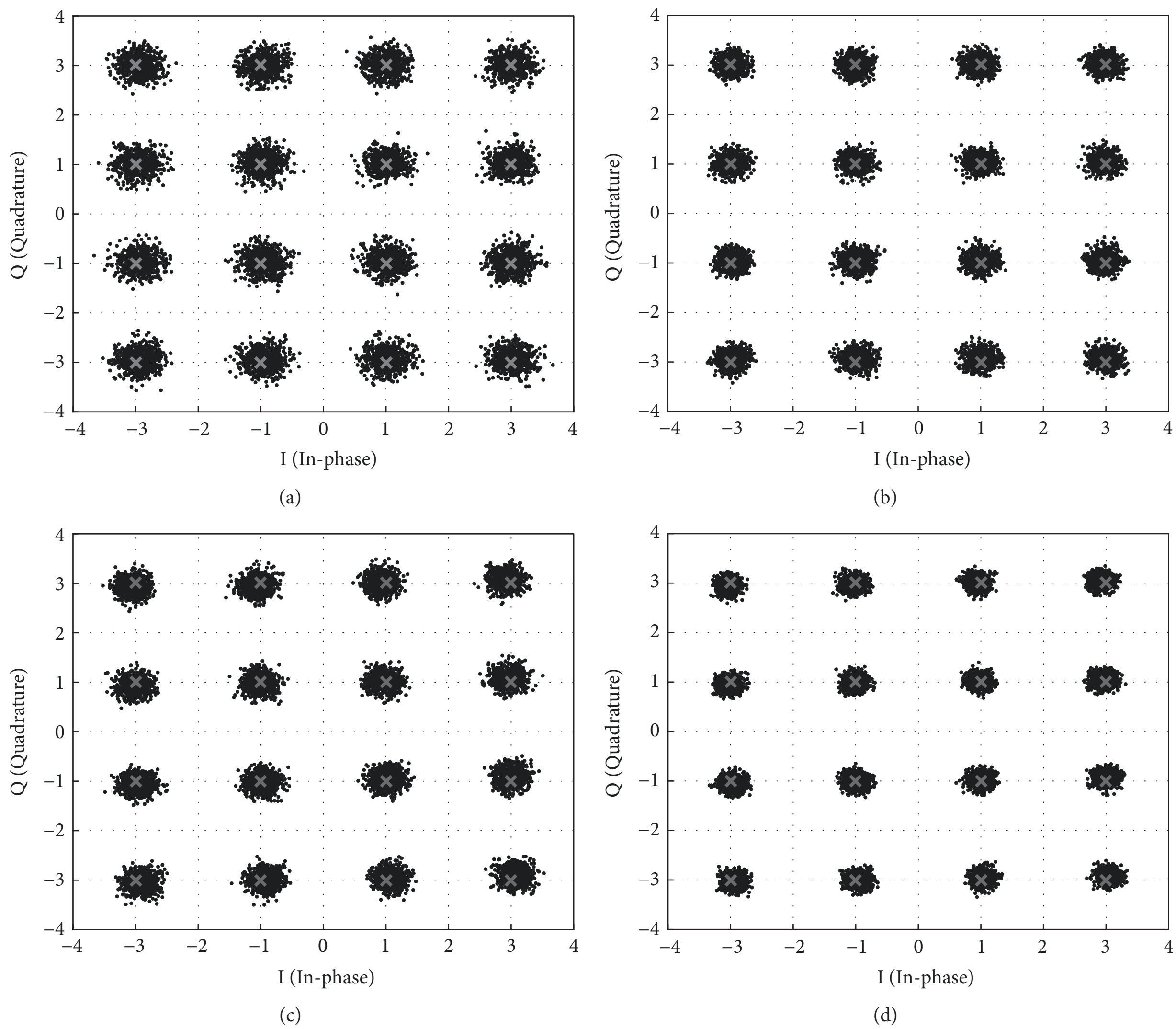

Figure 9: CMA-PTRBFNN and FC-CNNE output constellations: (a) CMA-PTRBFNN, Brazil D channel, (b) FC-CNNE, Brazil D channel, (c) CMA-PTRBFNN, Brazil E channel, and (d) FC-CNNE, Brazil E channel.

been carefully defined to achieve satisfactory control of the FC-CNNE adaptation steps.

The proposed equalizer has been implemented in a 16-QAM system using C programming language. The equalizer performance has been evaluated over five benchmark multipath scenarios, defined by the International Telecommunication Union, in terms of residual MSE, convergence rate, and BER. Results of the proposed FC-CNNE were compared to CMA-PTRBFNN. The results show that the proposed approach has significantly improved performance, achieving a faster convergence rate and lower residual steady-state MSE for the channel delay profiles Brazil B, Brazil C, and Brazil E. Consequently, the lower residual MSE resulted in a lower BER. For Brazil A channel, the residual MSE and BER for both equalizers are similar and the proposed equalizer presents a faster convergence rate. For Brazil D channel, the convergence rates are similar for both equalizers, with the proposed equalizer presenting a reduced residual MSE and BER.

Both equalizers last ten thousand output IQ symbols have been graphically depicted for the two most dispersive multipath scenarios (Brazil D and Brazil E channels). Results show that, for both cases, the output constellation of the proposed equalizer presents small dispersion around the IQ symbols of the reference constellation when compared to CMA-PTRBFNN.

It is known that the good performance of an adaptive channel equalizer is related to the appropriate selection of the equalizer parameters, such as the adaptation step and the filter coefficients initialization procedure. Thus, parameter selection in adaptive channel equalizers must be carefully considered, not only for wireless applications but also for the latest generations of single-carrier coherent optical receivers.

For future works, the authors intend to redesign the fuzzy block as a neuro-fuzzy system, such that the FC block would not require a specialist knowledge, being able

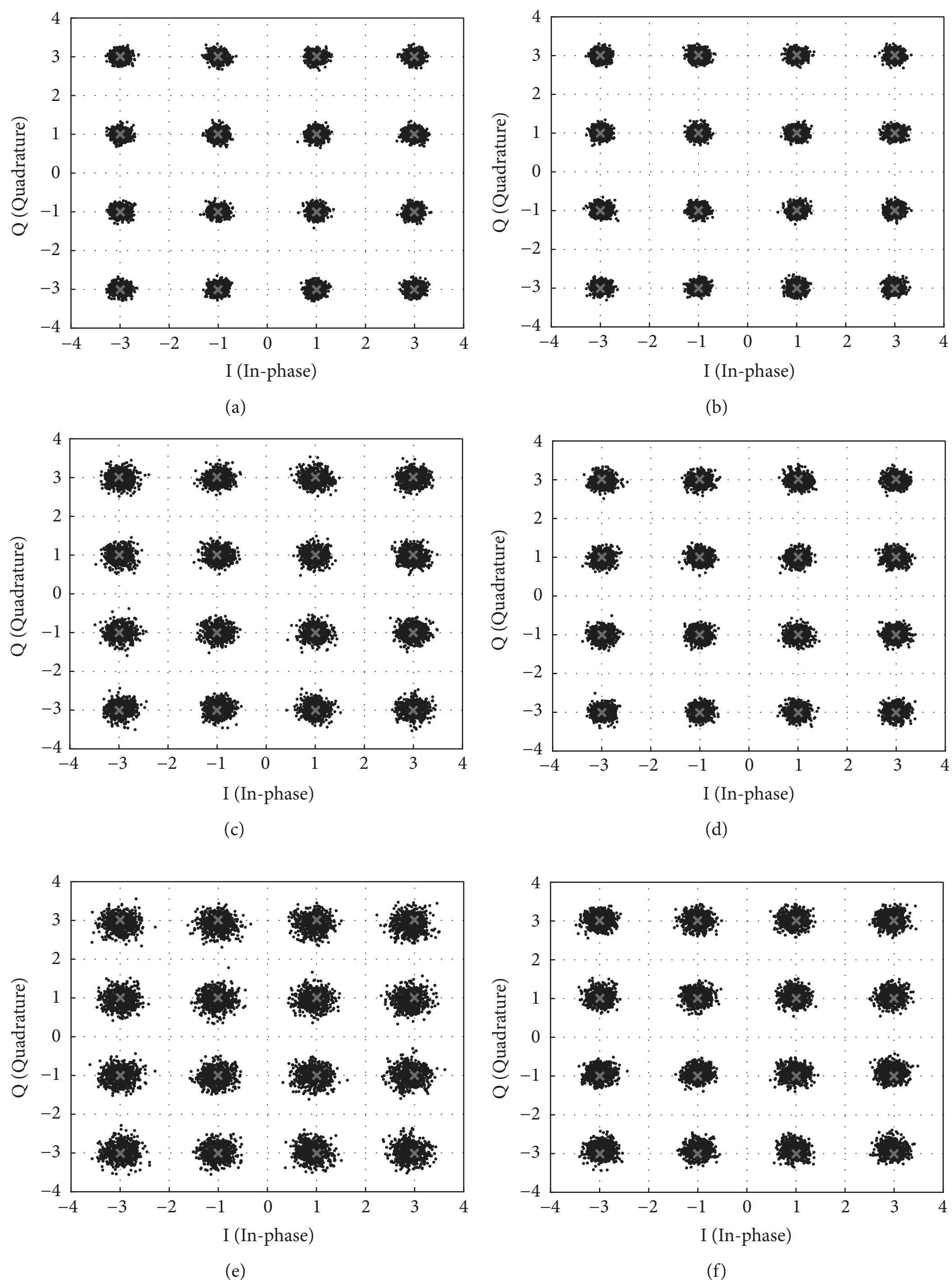

Figure 10: CMA-PTRBFNN and FC-CNNE output constellations: (a) CMA-PTRBFNN, Brazil A channel, (b) FC-CNNE, Brazil A channel, (c) CMA-PTRBFNN, Brazil B channel, (d) FC-CNNE, Brazil B channel, (e) CMA-PTRBFNN, Brazil C channel, and (f) FC-CNNE, Brazil C channel.

to achieve a satisfactory performance via a self-learning structure. Another possibility is to evaluate the use of the proposed FC-CNNE in order to mitigate chromatic and polarization mode dispersion in single-carrier coherent optical receivers.

Appendix

Figure 10 presents the Brazil A, B, and C constellation and outputs for CMA-PTRBFNN and FC-CNNE. The proposed FC-CNNE has smaller dispersions around the reference symbols than the CMA-PTRBFNN, which resulted in the better MSE results.

Data Availability

The data used to support the findings of this study are available from the corresponding author upon request.

Conflicts of Interest

The authors declare that they have no conflicts of interest.

Acknowledgments

This study was financed in part by the Coordenação de Aperfeiçoamento de Pessoal de Nível Superior—Brasil (CAPES)—Finance Code 001.

References

[1] A. Khare, K. Trivedi, and S. Dixit, "Effect of Doppler frequency and ber in FFT based OFDM system with Rayleigh fading channel," in *Proceedings of the 2014 IEEE Students' Conference on Electrical, Electronics and Computer Science, SCEECS 2014*, March 2014.

[2] D. V. Loss, M. C. F. Decastro, P. R. G. Franco, and F. C. C. Decastro, "Phase transmittance RBF neural networks," *IEEE Electronics Letters*, vol. 43, no. 16, pp. 882–884, 2007.

[3] Z. Zerdoumi, D. Chikouche, and D. Benatia, "Adaptive decision feedback equalizer based neural network for nonlinear channels," in *Proceedings of the 2013 3rd International Conference on Systems and Control, ICSC 2013*, pp. 850–855, October 2013.

[4] S. Chen, "Low complexity concurrent constant modulus algorithm and soft decision directed scheme for blind equalisation," *IEE Proceedings Vision, Image and Signal Processing*, vol. 150, no. 5, pp. 312–320, 2003.

[5] H. K. Sahoo and B. Mohanty, "Adaptive decision feedback equalizer for SISO communication channel using combined FIR-neural network and fast block LMS algorithm," in *Proceedings of the 2016 IEEE Annual India Conference, INDICON 2016*, pp. 1–5, December 2016.

[6] S. Das, "Design of adaptive channel equaliser on neural framework using fuzzy logic based multilevel sigmoid slope adaptation," in *Proceedings of the International Conference on Signal Processing Communications and Networking, ICSCN 2008*, pp. 274–278, January 2008.

[7] S. Haykin, *Adaptive Filter Theory*, Prentice-Hall, Upper Saddle River, NJ, USA, 3rd edition, 1996.

[8] A. D. Beikos and A. P. Liavas, "Performance analysis and comparison of blind to non-blind least-squares equalization with respect to effective channel overmodeling," *Signal Processing*, vol. 82, no. 9, pp. 1233–1253, 2002.

[9] F. C. C. De Castro, M. C. F. De Castro, and D. S. Arantes, "Concurrent blind deconvolution for channel equalization," *IEEE International Conference on Communications*, vol. 2, pp. 366–371, 2001.

[10] D. N. Godard, "Self-recovering equalization and carrier tracking in two-dimensional data communication systems," *IEEE Transactions on Communications*, vol. 28, no. 11, pp. 1867–1875, 1980.

[11] J. G. Proakis and M. Salehi, *Digital Communications*, vol. 5, McGraw-Hill, 4th edition, 2008.

[12] O. Macchi and E. Eweda, "Convergence Analysis of Self-Adaptive Equalizers," *IEEE Transactions on Information Theory*, vol. 30, no. 2, pp. 161–176, 1984.

[13] S. Chen, B. L. Luk, C. J. Harris, and L. Hanzo, "Fuzzy-logic tuned constant modulus algorithm and soft decision-directed scheme for blind equalisation," *Digital Signal Processing*, vol. 20, no. 3, pp. 846–859, 2010.

[14] C.-C. Yeh and J. R. Barry, "Adaptive minimum bit-error rate equalization for binary signaling," *IEEE Transactions on Communications*, vol. 48, no. 7, pp. 1226–1235, 2000.

[15] X. Y. Hu, C. M. Zhao, J. Ding, and X. H. Yu, "Simplified fuzzy stochastic gradient FIR adaptive equalizer for terrestrial HDTV transmission," *IEEE Transactions on Consumer Electronics*, vol. 43, no. 4, pp. 1090–1099, 1997.

[16] Y. H. Ng, H. Mohamad, and T. C. Chuah, "Block-based fuzzy step size NLMS algorithms for subband adaptive channel equalisation," *IET Signal Processing*, vol. 3, no. 1, pp. 23–32, 2009.

[17] L. A. Zadeh, "Outline of new approach to the analysis of complex systems and decision processes," *IEEE Transactions on Systems, Man, and Cybernetics*, vol. 3, pp. 28–44, 1973.

[18] E. H. Mamdani, "Application of fuzzy algorithms for the control of a simple dynamic plant," *Proceedings of the IEEE*, vol. 121, no. 12, pp. 1585–1588, 1974.

[19] R. D. Gitlin and S. B. Weinstein, "Fractionally-Spaced Equalization: An Improved Digital Transversal Equalizer," *Bell System Technical Journal*, vol. 60, no. 2, pp. 275–296, 1981.

[20] 2018, https://www.itu.int/pub/R-REP-BT.2035-2-2008/.

[21] T. J. Endres, *Equalizing with Fractionally-Spaced Constant Modulus And Second-Order-Statistics Blind Receivers [Ph.D. Thesis]*, Cornell University, Ithaca, NY, USA, 1997.

[22] J. Bóveda, G. Marcos, J. M. Pérez, S. Ponce, and A. Aranaz, "MER degradation in a broadcast mobile network," in *Proceedings of the 2009 IEEE International Symposium on Broadband Multimedia Systems and Broadcasting, BMSB 2009*, pp. 1–5, May 2009.